# Three-dimensional image realization in interference microscopy

Stanley S. C. Chim and Gordon S. Kino

We describe an efficient algorithm based on the Hilbert transform for reconstructing cross-sectional or three-dimensional images from the input images acquired by an interference microscope. First the design of this filter is presented, and cross-sectional images of an integrated circuit constructed with this algorithm are demonstrated. It is shown that this Hilbert transform algorithm can be easily implemented with a low-cost frame grabber so that the computation time required for image reconstruction is drastically reduced.

## Introduction

In this paper we describe a fast algorithm for reconstructing cross-sectional images from the interference images acquired by an optical interference microscope. A Mirau correlation microscope, based on the Mirau interferometer configuration, is employed in our experiments.[1–3] The schematic of the microscope is shown in Fig. 1. A spatially and temporally incoherent light source from a xenon arc lamp collimated by a condenser fills the back focal plane of a microscope objective. A Mirau interferometer consisting of a beam splitter and a reference mirror is positioned between the objective and the sample. The reference mirror is always kept at the focal plane ($z = 0$) of the objective, while the sample is scanned axially (along the $z$ axis) by a computer-controlled piezoelectric pusher in $N_{\text{scan}} = 64$ steps of size $\Delta z$. Thus at the $n$th step, the sample is located at an axial location $n\Delta z$, measured from the focal plane $z = 0$. A CCD camera is used to capture image signals in the form of interference fringes at each step. These fringes are the results of the cross correlation of the reflected signals from the reference mirror (signal $B$) and from the sample (signal $A$). The image acquired by the CCD camera can be expressed in the form

$$I_{xy}(n\Delta z) = A_{xy}{}^2 + B^2 + 2A_{xy}B\gamma_{xy}(n\Delta z). \quad (1)$$

A mathematical form for the cross correlation $\gamma_{xy}(n\Delta z)$ has been worked out for both broadband and single-frequency illumination.[3] The correlation term $\gamma_{xy}(n\Delta z)$ can be approximated by an envelope function $g_{xy}(n\Delta z)$ with a cosine phase variation $\Phi_{xy}(n\Delta z)$;

$$\gamma_{xy}(n\Delta z) \sim g_{xy}(n\Delta z)\cos[\Phi_{xy}(n\Delta z)]. \quad (2)$$

An interference image acquired by a CCD camera [Eq. (1)] is not easy to interpret owing to the presence of bright and dark fringes. One way to eliminate the interference fringes is by filtering the image data along the axial axis or the $z$ axis. In our earlier work,[3] we first carried out a Fourier transform on the input images [Eq. (1)] in the z direction for each $(x, y)$ location. Since the sample is scanned in $N_{\text{scan}} = 64$ steps in our experiment, we have an $N_{\text{scan}} = 64$-point Fourier transform. The zero frequency component and the negative frequency components are eliminated in the spatial frequency domain, and the inverse transform of the result is then taken. From Fourier transform theory,[4] it is clear that this process eliminates the background bias $(A_{xy}{}^2 + B^2)$ in Eq. (1), and Eq. (1) is now transformed to a function $V_{xy}(n\Delta z)$ with a single sideband:

$$V_{xy}(n\Delta z) = 2A_{xy}Bg_{xy}(n\Delta z)\exp[j\Phi_{xy}(n\Delta z)]. \quad (3)$$

Since the transformed image $V_{xy}(n\Delta z)$ contains an exponential phase variation, the fringes caused by the sinusoidal phase variations in the interference images are now removed. However, this algorithm requires filtering the image data in the frequency domain; it thus requires two Fourier transforms (forward and inverse) along the $z$ direction for each pixel $(x, y)$ on the sample. Consequently, a large amount of memory and processing time is required

The authors are with the Edward L. Ginzton Laboratory, Stanford University, Stanford, California 94305-4085.

Received 22 January 1991.
0003-6935/92/142550-04$05.00/0.

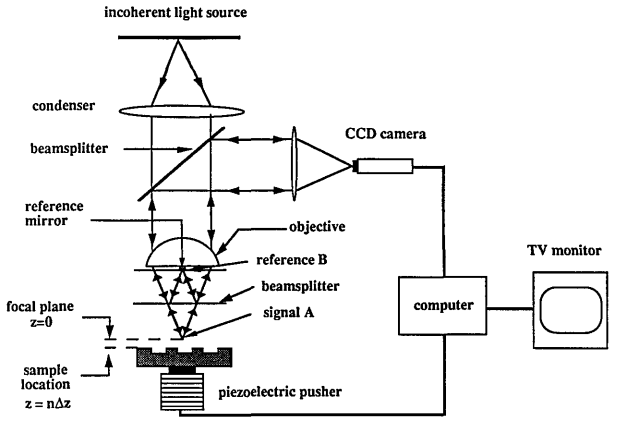


Fig. 1. Schematic of the Mirau correlation microscope.

for the reconstruction of a 128 × 128 pixel cross-sectional image. It is thus difficult to realize real-time cross-sectional imaging with an algorithm that operates on a pixel-by-pixel basis. In this paper the Hilbert transform algorithm is introduced as a short cut for producing two-dimensional cross-sectional images. This technique has two advantages. First, only a limited number of image planes (typically as few as eight; see the next section) are needed for transformation to produce one cross-sectional image. Second, the transformation required can be carried out with standard image capture board hardware[5] in a parallel processing mode.

### Hilbert Transform

The input image $I_{xy}(n\Delta z)$ acquired by an interference microscope has a cosine phase variation, as illustrated in Eq. (1) and expression 2. The desired image $V_{xy}(n\Delta z)$ [Eq. (3)], however, has an exponential phase variation with the same argument $\Phi_{xy}(n\Delta z)$. Clearly, an alternative method to obtain $V_{xy}(n\Delta z)$ is first to subtract the background bias $(A_{xy}^2 + B^2)$ from the input image $I_{xy}(n\Delta z)$ to form an unbiased image $i_{xy}(n\Delta z)$ and then to construct a $\pi/2$ phase-shifted image $i_{xy}^*(n\Delta z)$ from $i_{xy}(n\Delta z)$ so that

$$V_{xy}(n) = i_{xy}(n) + j i_{xy}^*(n), \tag{4}$$

where

$$i_{xy}(n) = I_{xy}(n) - (A_{xy}^2 + B^2) = 2A_{xy}Bg_{xy}(n)\cos[\Phi_{xy}(n)], \tag{5}$$

$$i_{xy}^*(n) = 2A_{xy}Bg_{xy}(n)\sin[\Phi_{xy}(n)], \tag{6}$$

with $j = \sqrt{-1}$. In order to keep the equations simple, the step size $\Delta z$ has not been written explicitly. The background bias image $(A_{xy}^2 + B^2)$ can easily be acquired by moving the reference mirror (Fig. 1) out of focus so that there is no interference between the signals from the sample and those from the reference mirror.

It has been shown that the phase-shifted signal $i_{xy}^*(n\Delta z)$ can be obtained from $i_{xy}(n\Delta z)$ by a Hilbert transform[6] whose frequency response $H(e^{j\omega})$ is given by

$$H[\exp(jw)] = \begin{cases} -j & 0 \le \omega < \pi \\ j & \pi \le \omega < 2\pi \end{cases}. \tag{7}$$

The angular frequency $\omega$ is defined as $2\pi k_z \Delta z$ where $\Delta z$ is the step size and $k_z$ is the spatial frequency along the $z$ axis. The impulse response $h(n)$ of the Hilbert transform is given by[6]

$$h(n) = \begin{cases} 2/\pi n & n \text{ odd} \\ 0 & \text{otherwise} \end{cases}. \tag{8}$$

The phase-shifted image $i_{xy}^*(n)$ is then calculated by convolving $h(n)$ with $i_{xy}(n)$.

The ideal frequency response of the Hilbert transform is plotted in Fig. 2. In practical terms, it is never possible to achieve the ideal response because an infinite number of filter elements are required to process the images along the $z$ axis. The responses of the finite-length filters shown in Fig. 2 illustrate the introduction of ripples into the ideal frequency response in a practical filter of finite length. It is observed that the maximum rippling introduced by a Hilbert filter with 19 elements is 16%. By choosing the sampling frequency close to the Nyquist rate, one can locate the spectrum of the cross-correlation signal close to the passband center of the Hilbert response, hence minimizing the effects of the ripples. It is

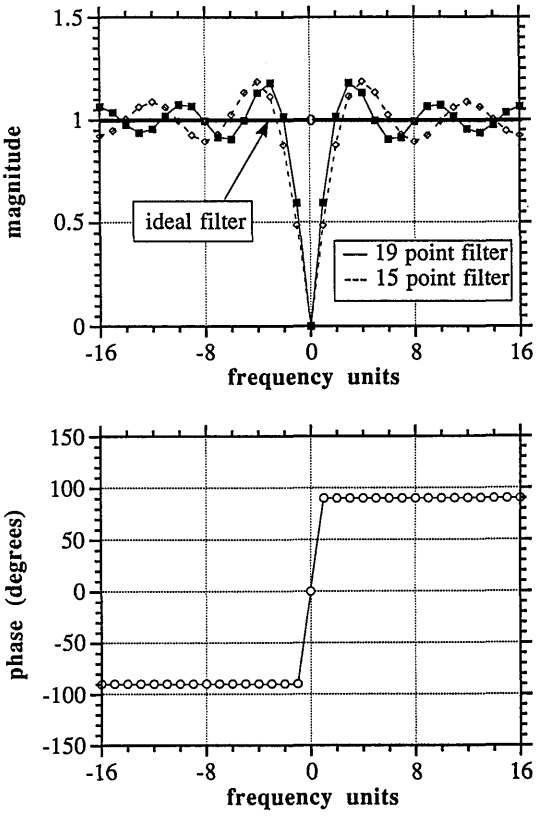


Fig. 2. Comparison between the frequency responses—(top) magnitude and (bottom) phase—of an ideal Hilbert filter (solid line) and those of finite length (solid and dashed curves).

convenient to define a normalized impulse response $h_{\text{norm}}(n)$ for a Hilbert transformer with $(2M + 1)$ elements, where

$$h_{\text{norm}}(n) = \begin{cases} \frac{1}{n} & \text{if } |n| \le M \text{ and } n \text{ is odd} \\ 0 & \text{otherwise} \end{cases} \tag{9}$$

The phase-shifted image $i_{xy}^*(n)$ is calculated by convolving $h(n)$ with $i_{xy}(n)$. Therefore we write

$$i_{xy}^*(n) = \frac{2}{\pi} \sum_{m=-M}^{m} i_{xy}(m - n) h_{\text{norm}}(m). \tag{10}$$

Since the impulse response $h_{norm}(n)$ is antisymmetric about $n = 0$ and it is zero for even $n$, Eq. (10) simplifies to

$$i_{xy}^*(n) = \frac{2}{\pi} \sum_{\substack{m=1 \\ m \text{ odd}}}^{M} \frac{i_{xy}(m - n) - i_{xy}(m + n)}{m}. \tag{11}$$

The number of nontrivial multiplications (or divisions in this case) involved in a $(2M + 1)$ point Hilbert transformer is $(M - 1)/2$, which is a factor of 4 less than that of most other finite impulse response digital filters,[6] as illustrated by Eq. (11). For our application, we have found that a 19-point Hilbert filter is sufficient (as shown in the next section), which involves just four nontrivial multiplications. The most important characteristic of the Hilbert transform, however, is that its normalized impulse response $h_{\text{norm}}(n)$ [Eq. (11)] values are just simple fractions (1, 1/3, 1/5, . . .), which makes it possible to use an 8-bit processor to do the arithmetic with reasonable accuracy. The simplicity of the filter coefficients enables us to use an 8-bit image capture board for the arithmetic, which works on a frame-by-frame basis instead of a repetitive execution, pixel by pixel. Hence it takes the Hilbert transform algorithm only one execution to produce an $M \times M$ cross-sectional image, while $M^2$ executions are required to produce the same image with an algorithm (such as our previous Fourier algorithm), which operates on a pixel-by-pixel basis. With a frame processing board capable of fast arithmetic operations, it may thus be possible to produce a real-time cross-sectional image from the interference images acquired by an interference microscope.

Once the phase-shifted image $i_{xy}^*(n)$ is calculated, the amplitude and phase of the desired image $V_{xy}(n)$ (Eq. 3) can readily be computed:

$$|V_{xy}(n)| = [[i_{xy}(n)]^2 + [i_{xy}^*(n)]^2]^{1/2},$$

$$\arg[V_{xy}(n)] = \tan^{-1}\left[\frac{i_{xy}^*(n)}{i_{xy}(n)}\right]. \tag{12}$$

### Amplitude Response $V(z)$

The amplitude response $V(z)$ of a microscope is obtained by placing a plane reflector at the object plane and recording the signal amplitude as the object is being moved out of focus. In our simulation for testing the Hilbert transform algorithm, we choose a 19-point Hilbert transformer and we limit ourselves to a 7-bit arithmetic. Figure 3(a) shows the simulated amplitude response $V(z)$ of the unprocessed signal and that obtained by the Hilbert filter for a scan distance of 3.0 μm along the $z$ axis. The simulated data obtained by the Fourier transform algorithm[2,3] are plotted as a series of crosses in Fig. 3(a) for comparison. The good agreement between these two filtered responses shows clearly that a 19-point Hilbert transformer is sufficient and that an 8-bit frame processor will not limit the accuracy of the filter. Figure 3(b) shows the experimental amplitude responses for the same scanned distance of 3.0 μm along the $z$ axis. Again there is good agreement between the filtered data obtained by the Fourier transform algorithm and those obtained by the Hilbert filter. The Hilbert filter is thus a fast alternate algorithm for extracting the correlation envelope from the interference fringes.

In our speed comparison test, we first acquired 64 images (each of size 128 × 128 pixels) as described previously. The time required to produce one cross-

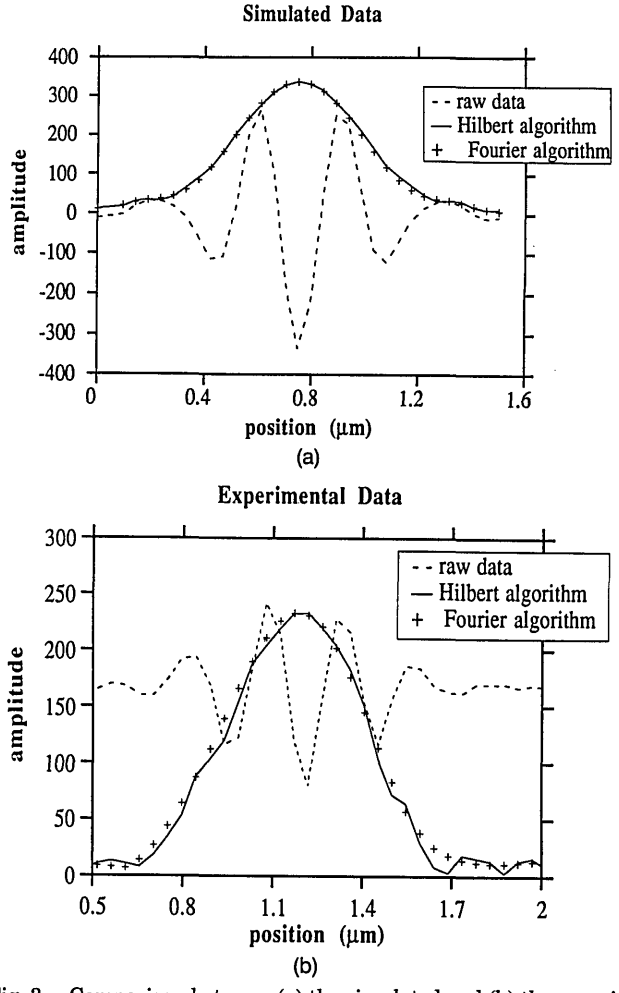


Fig. 3. Comparison between (a) the simulated and (b) the experimental amplitude responses of the unprocessed signal and those obtained by the Hilbert and Fourier transform algorithms.

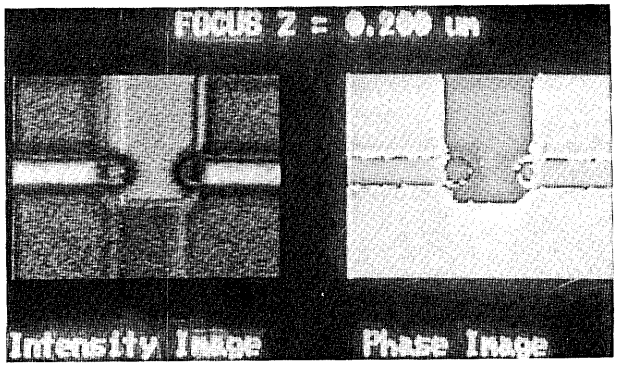


(a)

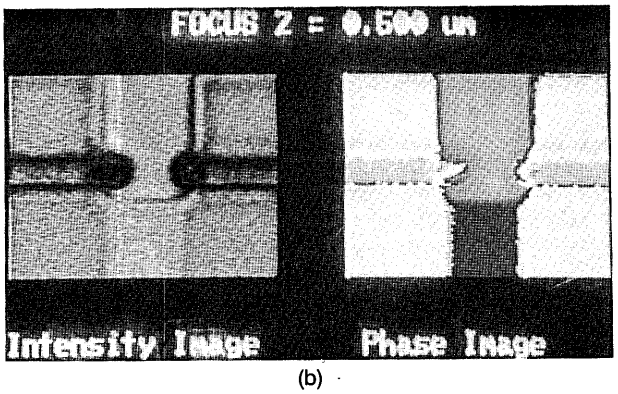


(b)

Fig. 4a. Intensity images of a multilayered (complementary metal-oxide semiconductor) integrated circuit at different foci [left, (a) and (b)]. The corresponding phase images of the same circuit [right, (a) and (b)].

sectional image from the 64 images (acquired by the CCD camera) with the Hilbert transformer is 12.6 s, compared with the 30 s required by our previous optimized fast-Fourier-transform algorithm.[2,3] The reduction in computation time is not as drastic as we would expect because the Hilbert transform algorithm is implemented using an image capture board, a Data Translation DT2851,[5] while the Fourier transform algorithm is implemented by using a 386 mathematical processor; since the image capture board runs significantly slower than the 386 processor, the speed comparison test favors the Fourier algorithm. However, if only an intensity image is required, all the filtering steps can be performed on the low-cost image capture board (Data Translation DT2851). The data processing time is now reduced to 10.5 s. Since the image capture board is operated on a frame-by-frame basis, the production of a square 256 × 256 pixel image will take approximately the same amount of computation time as a 128 × 128 square image. As we work with larger images, the Hilbert transform, which can be implemented by frame operations, will become much more efficient than algorithms, which have to operate on a pixel-by-pixel basis.

### Cross-Sectional Images of an Integrated Circuit

To illustrate the reconstruction of two-dimensional cross-sectional images from the raw data, a multilayered silicon integrated circuit complimentary metal-oxide semiconductor (cmos), was scanned along the $z$ axis for a distance of 3.2 μm. Signals were frame grabbed at 64 equally spaced vertical positions of the circuit and then processed by the Hilbert algorithm. Figure 4(a) shows four such intensity cross-sectional images at different foci. Each image is of size 128 × 128 pixels. As we scan along the $z$ axis, different regions of the circuit come into focus at different axial locations. By registering the values of $z$ of the intensity maxima for each region, we can construct the three-dimensional profile of the circuit. The corresponding phase images, shown in Fig. 4(b), are obtained as a by-product of the Hilbert algorithm. Since the height variations in our complimentary metal-oxide semiconductor circuit are more than a wavelength, the phase images suffer from ambiguous $2\pi$ phase wraparounds that make them hard for us to interpret. With both the phase and intensity (and hence the amplitude) images, it is easy to design an inverse filter for image enhancement, if so desired.

### Conclusions

In this paper we have presented an algorithm based on the Hilbert transform for processing the interference images collected by an interference microscope. Since this algorithm can take advantage of the frame processing capability of an image capture board, it is faster than any other algorithm that has to work on a pixel-by-pixel basis. With a low-cost frame grabber, we can produce a 256 × 256 pixel, square intensity image from the raw input data in less than 13 s.

This work was supported by International Business Machines on contract 645416.

### References

1. S. S. C. Chim, P. A. Beck, and G. S. Kino, "A novel thin film interferometer," Rev. Sci. Instrum. **61,** 980–983 (1990).
2. S. S. C. Chim and G. S. Kino, "Correlation microscope," Opt. Lett. **15,** 579–581 (1990).
3. G. S. Kino and S. S. C. Chim, " The Mirau correlation microscope," Appl. Opt. **29,** 3775–3783 (1990).
4. R. N. Bracewell, *The Fourier Transform and Its Applications,* 2nd ed. (McGraw-Hill, New York, 1986).
5. *Image Processing Handbook,* Rep. No. 20-07373-3 (Data Translation, Inc., Marlboro, Mass., 19902).
6. L. R. Rabiner and B. Gold, *Theory and Application of Digital Signal Processing* (Prentice-Hall, Englewood Cliffs, N.J., 1975).